



Available online at www.sciencedirect.com



ScienceDirect

Trans. Nonferrous Met. Soc. China 35(2025) 863–871

Transactions of
Nonferrous Metals
Society of China

www.tnmsc.cn



Creep-fatigue lifetime prediction of GH720Li superalloy considering effect of grain size

Bin ZHANG¹, Rong-qiao WANG^{2,3,4}, Dian-yin HU^{2,3,4}, Hong-bo LI⁵, Kang-he JIANG⁶, Jia-ming WEI⁷, Hong ZHANG⁸

1. Hangzhou International Innovation Institute, Beihang University, Hangzhou 311115, China;
2. Research Institute of Aero-engine, Beihang University, Beijing 100191, China;
3. Beijing Key Laboratory of Aero-engine Structure and Strength, Beijing 100191, China;
4. United Research Center of Mid-Small Aero-engine, Beijing 100191, China;
5. School of Aerospace Engineering, Tsinghua University, Beijing 100084, China;
6. Hunan Aviation Powerplant Research Institute, Aero Engine (Group) Corporation of China, Zhuzhou 412002, China;
7. Hangzhou Turbine Power Group Co., Ltd., Hangzhou 310000, China;
8. Failure Mechanics and Engineering Disaster Prevention, Key Laboratory of Sichuan Province, Sichuan University, Chengdu 610065, China

Received 12 August 2023; accepted 22 March 2024

Abstract: In order to accurately evaluate the creep-fatigue lifetime of GH720Li superalloy, a lifetime prediction model was established, reflecting the interaction between creep damage and low-cycle fatigue damage. The creep-fatigue lifetime prediction results of GH720Li superalloy with an average grain size of 17.3 μm were essentially within a scatter band of 2 times, indicating a strong agreement between the predicted lifetimes and experimental data. Then, considering that the grain size of the dual-property turbine disc decreases from the rim to the center, a grain-size-sensitive lifetime prediction model for creep-fatigue was established by introducing the ratio of grain boundary area. The improved model overcame the limitation of most traditional prediction methods, which failed to reflect the relationship between grain size and creep-fatigue lifetime.

Key words: creep-fatigue; lifetime prediction; GH720Li superalloy; grain size; damage accumulation

1 Introduction

Due to the excellent mechanical performance, including strength, fatigue resistance, and creep resistance at elevated temperatures, GH720Li superalloy has been successfully employed in aero-engine turbine discs [1–3]. Due to the high temperatures and cyclic centrifugal forces experienced during repeated engine operations, turbine discs are subjected to significant creep-fatigue damage, which is one of the primary reasons for turbine disc failure [4,5]. Therefore, accurate prediction of the creep-fatigue lifetime for GH720Li

superalloy is particularly significant in the gas turbine industry.

The creep-fatigue performance of nickel-based superalloys is closely related to various factors, including temperature [6], mechanical loading [7–9], frequency [10], dwell time, and dwell position [4,5,11,12]. In addition, the heat treatment process and grain size could affect the mechanical properties of materials [13–15], and they have been confirmed to have significant effects on creep-fatigue properties. JACKSON and REED [16] investigated the microstructure evolution of Udimet 720Li superalloy (similar to GH720Li superalloy in China) during various heat treatment processes and

Corresponding author: Dian-yin HU, Tel: +86-10-82313841, E-mail: hdy@buaa.edu.cn

DOI: [https://doi.org/10.1016/S1003-6326\(24\)66719-1](https://doi.org/10.1016/S1003-6326(24)66719-1)

1003-6326/© 2025 The Nonferrous Metals Society of China. Published by Elsevier Ltd & Science Press

This is an open access article under the CC BY-NC-ND license (<http://creativecommons.org/licenses/by-nc-nd/4.0/>)

found that the duration of heat treatment significantly influenced the fatigue resistance of nickel-based superalloys. Creep-fatigue experiments conducted on Udimet 720Li superalloy with varying grain sizes revealed that the grain size was one of the primary factors influencing creep-fatigue performance [17]. At 650 °C in air, a larger grain size was beneficial to resisting crack growth and improving creep-fatigue performance [17]. CHEN et al [18] conducted creep-fatigue experiments on GH230 superalloy, and the results indicated that local deformation inhomogeneity at the crystal scale of the material could lead to intergranular damage.

According to continuum damage mechanics, creep-fatigue damage is caused by the accumulation of creep damage and low-cycle fatigue damage, and damage-based lifetime prediction models have been widely used in creep-fatigue lifetime prediction [19–21]. Furthermore, based on the nonlinear damage accumulation theory, BERTI and MONTI [22] and WANG et al [23] developed creep-fatigue lifetime prediction models considering temperature variations. The material constants in these models can be obtained from experimental data on creep and low-cycle fatigue, thus reducing the need for a large number of expensive creep-fatigue experiments. Although fruitful studies on creep-fatigue lifetime prediction for nickel-based superalloys have been conducted, few damage-based lifetime prediction models consider the influence of grain size on creep-fatigue lifetimes.

In this regard, the present study focused on developing a damage-based creep-fatigue lifetime prediction model for GH720Li superalloy considering the effect of grain size. Firstly, based on the creep-fatigue damage mechanism and nonlinear damage accumulation theory, the evolution of creep-fatigue damage was characterized, and a damage-based creep-fatigue lifetime prediction model for GH720Li superalloy was established. Then, considering the effect of grain size on creep-fatigue damage, an improved grain-size-sensitive damage model of creep-fatigue was innovatively developed. Finally, without introducing any additional material constants, the predicted creep-fatigue lifetimes of GH720Li superalloy fell within a scatter band of 2 times, and the predicted relationship between creep-fatigue lifetimes and grain sizes was in good agreement with the experimental data.

2 Damage-based lifetime prediction model

2.1 Creep-fatigue damage characterization

Generally, the contribution of the interaction between creep damage and low-cycle fatigue damage determines the creep-fatigue lifetimes [21,24,25]. When the dwell time is relatively short, even at high temperatures, the creep-fatigue damage behavior is similar to low-cycle fatigue damage behavior, which exhibits transgranular fracture characteristics in polycrystalline materials [26,27]. With increasing dwell time, the creep damage gradually increases until the failure mode approaches pure creep. A typical creep damage mechanism involves microvoids nucleating and growing into macroscopic intergranular cracks at grain boundaries in high-temperature environments due to the weakness of these boundaries [28,29]. The fractographic analysis following creep-fatigue experiments on GH720Li superalloy in previous studies [5] revealed a mixed transgranular and intergranular fracture mode, with intergranular fracture becoming more pronounced with increasing dwell time.

The creep-fatigue lifetimes can be predicted through coupling creep damage and low-cycle fatigue damage [19–21]. As shown in Fig. 1, ductility exhaustion methods typically use a linear creep-fatigue interaction assumption, while the ASME code uses a bilinear creep-fatigue interaction assumption [30]. Furthermore, a growing number of studies have shown that describing creep-fatigue damage based on nonlinear damage accumulation theory is effective [21].

KACHANOV [31] formulated an equation

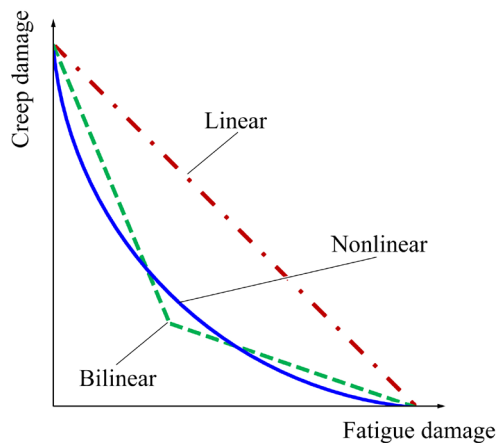


Fig. 1 Schematic diagram of three methods for describing creep-fatigue damage

describing the evolution of creep damage in terms of stress and cumulative damage:

$$dD_c = \left(\frac{\sigma}{A(1-D_c)} \right)^r dt \quad (1)$$

where D_c is the creep damage, σ is the stress, t is time, and A and r are the temperature-related material constants. Based on the pioneering work of KACHANOV [31], an improved evolution equation for creep damage was proposed by introducing an additional material constant (m) [32,33]:

$$dD_c = \left(\frac{\sigma}{A} \right)^r (1-D_c)^{-m} dt \quad (2)$$

For low-cycle fatigue damage, a classic evolution equation has been widely used for predicting lifetimes under complex loads [34]:

$$dD_f = \left(\frac{\sigma_a}{M} \right)^\beta (1-D_f)^{-b} dN \quad (3)$$

where D_f is the low-cycle fatigue damage, σ_a is the stress amplitude, N is the number of cycles, and β , M and b are the temperature-related material constants.

In creep-fatigue, the damage from creep and low-cycle fatigue is coupled and mutually promotes each other [6,21,22]. In this work, the interaction between creep damage (described by Eq. (2)) and low-cycle fatigue damage (described by Eq. (3)) was reflected through the nonlinear damage accumulation theory. The creep-fatigue damage D could be expressed as [7]

$$dD = \left(\frac{\sigma}{A} \right)^r (1-D)^{-m} dt + \left(\frac{\sigma_a}{M} \right)^\beta (1-D)^{-b} dN \quad (4)$$

By integrating creep damage over a cycle, the first derivative of the total creep-fatigue damage with respect to the number of cycles can be expressed as

$$\frac{dD}{dN} = (1-D)^{-m} \int_{t_1}^{t_2} \left(\frac{\sigma}{A} \right)^r dt + (1-D)^{-b} \left(\frac{\sigma_a}{M} \right)^\beta \quad (5)$$

where t_1 and t_2 are the start and end time of the dwell load in a cycle, respectively.

2.2 Application of damage-based lifetime prediction model in creep-fatigue

By fitting the experimental data of creep and low-cycle fatigue of GH720Li superalloy, the material constants for creep damage and low-cycle fatigue damage in the creep-fatigue lifetime prediction model can be determined. the creep and low-cycle fatigue experimental data of GH720Li superalloy at 650 °C were provided in Ref. [35]. All the material constants in the lifetime prediction model of GH720Li superalloy at 650 °C were listed in Table 1. As depicted in Fig. 2, the fitting results for both the creep and low-cycle fatigue lifetimes of GH720Li superalloy fell within a scatter band of 2 times, indicating a strong correlation between the predicted lifetimes and experimental data.

For GH720Li superalloy with an average grain size of 17.3 μm, the experimental creep-fatigue lifetimes were provided in Ref. [36]. Based on the damage-based lifetime prediction model (Eq. (5)) and the material constants obtained in this paper (Table 1), the creep-fatigue lifetimes of GH720Li superalloy at 650 °C were predicted. Majority of the agreements between the predicted results and experimental results of the creep-fatigue lifetimes of GH720Li superalloy were basically within a scatter band of 2 times (Fig. 3), verifying the accuracy of the creep-fatigue lifetime prediction model developed in this paper.

It was worth noting that stress amplitude conversion was necessary in creep-fatigue lifetime prediction. During the identification process of material constants, low-cycle fatigue experimental data at 650 °C from Ref. [35] were obtained under cyclic loading with a load ratio of $R=-1$. However, the creep-fatigue experiments in Ref. [36] were conducted under cyclic loading with a load ratio of $R=0.1$. Considering the difference of the load ratio, during the progress of creep-fatigue lifetime prediction, the stress amplitude at $R=0.1$ ($\sigma_{a(R=0.1)}$) in creep-fatigue experiments was converted into stress amplitude at $R=-1$ ($\sigma_{a(R=-1)}$) through the Goodman function [37]:

Table 1 Material constants in lifetime prediction model of GH720Li superalloy at 650 °C

Creep damage constant			Low-cycle fatigue damage constant		
m	A	r	b	M	β
43.0246	1854.1287	12.4305	40.0368	2357.2896	12.5659

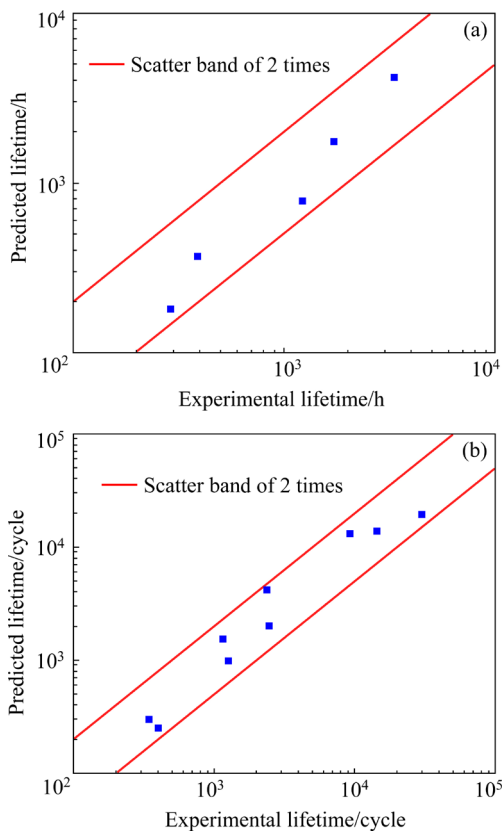


Fig. 2 Comparison of experimental and predicted lifetimes of GH720Li superalloy at 650 °C: (a) Creep lifetime; (b) Low-cycle fatigue lifetime

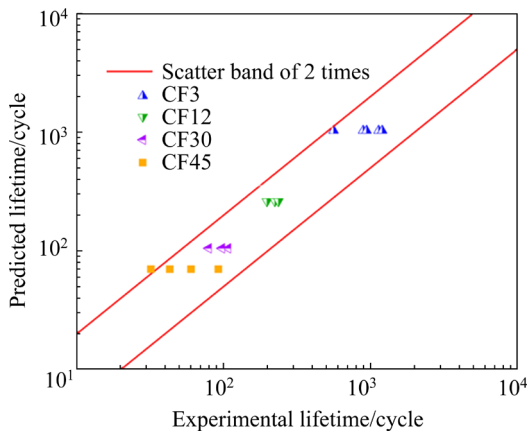


Fig. 3 Correlation between predicted and experimental creep-fatigue lifetimes of GH720Li superalloy at 650 °C (CF3, CF12, CF30 and CF45 indicate that the dwell time at the maximum load is 3, 12, 30 and 45 min, respectively)

$$\sigma_{a(R=0.1)} = \frac{\sigma_{a(R=0.1)}}{(1 - \sigma_m/\sigma_b)} \quad (6)$$

where σ_m and σ_b are the mean stress and ultimate stress, respectively. For GH720Li superalloy, σ_b at 650 °C is 1420 MPa [35].

3 Lifetime prediction considering effect of grain size

3.1 Grain-size-sensitive damage model of creep-fatigue

With the advancement of high thrust-weight ratio aero-engines, the service environment of turbine discs deteriorates continuously, and the material property requirements in different parts of the turbine disc exhibit significant differences [38,39]. Under this background, the dual-property turbine disc (Fig. 4) has gradually developed. In the dual-property turbine disc, the creep resistance decreases from the rim to the center as the grain size diminishes, while the evolution of low-cycle fatigue resistance follows the opposite trend [38,39]. Most traditional creep-fatigue lifetime prediction methods currently fail to reflect the relationship between grain size and lifetime. An important goal of this study is to establish a grain-size-sensitive creep-fatigue damage model without introducing any additional material constants.

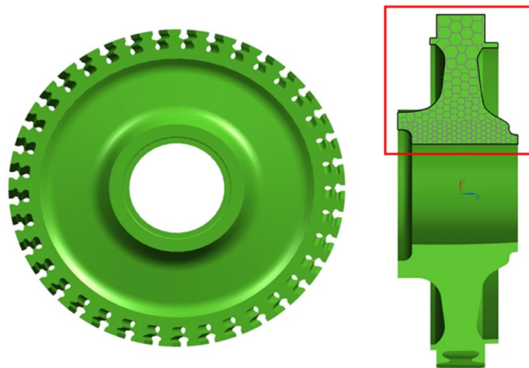


Fig. 4 Schematic diagram of dual-property turbine disc

Under creep-fatigue loading, intergranular fractures caused by creep damage and transgranular fractures caused by low-cycle fatigue damage occur simultaneously [5,36]. However, the effects of grain size on creep damage and low-cycle fatigue damage are quite different. As shown in Fig. 5, when the grain size decreases, the total area of grain boundary increases, which would result in more initiation of intergranular cracks and more serious creep damage [27]. However, studies have shown that low-cycle fatigue damage decreases with decreasing grain size due to the hindrance of grain boundaries on transgranular crack propagation [40–42]. Overall, as the grain size decreases, creep damage

increases, while low-cycle fatigue damage decreases. And the effect of grain size on creep damage and low-cycle fatigue damage is closely related to the total grain boundary area.

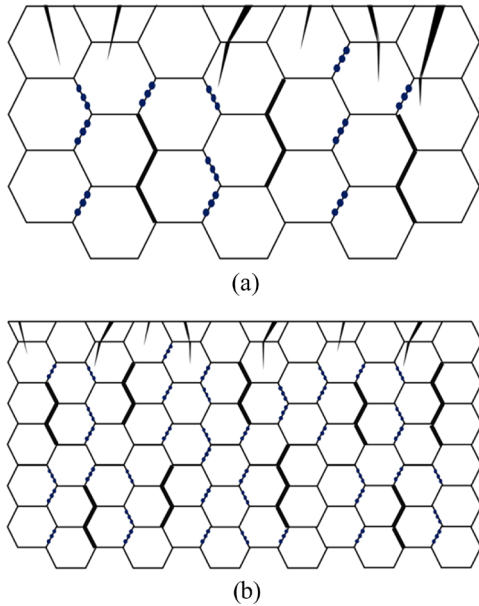


Fig. 5 Schematic diagrams of creep-fatigue damage mechanism under different grain sizes: (a) Large grain size; (b) Small grain size (The regular hexagons represent grains; the spots represent the micro-voids in growth; the black fold lines at grain boundaries represent intergranular cracks; the black fold lines passing through the grains represent transgranular cracks)

For the gauge part of the specimen with volume V_0 , the number of crystal grains (n) is

$$n = \frac{V_0}{V_{\text{grain}}(l^3)} \quad (7)$$

where l represents the grain size, and $V_{\text{grain}}(l^3)$ denotes the average volume of a single grain, which is proportional to the cube of the grain size. The total grain boundary area (S) in the gauge part of the specimen is proportional to the number of crystal grains and the effective grain boundary area within a single grain:

$$S \propto n S_{\text{grain}}(l^2) \quad (8)$$

where $S_{\text{grain}}(l^2)$ indicates the effective grain boundary area within a single grain, which is proportional to the square of grain size. After simplification, Eq. (8) could be described as

$$S \propto \frac{1}{l} \quad (9)$$

Selecting the total grain boundary area at a specific grain size as a reference, the ratio of the total grain boundary area to the reference total grain boundary area (η) can be expressed as

$$\eta = \frac{S}{S_0} = \frac{l_0}{l} \quad (10)$$

where S_0 and l_0 are the reference total grain boundary area and reference grain size, respectively. The grain boundary area can be accurately measured by some advanced technology [43], and then η can also be obtained based on Eq. (10).

In this work, to reflect the influence of grain size on creep-fatigue lifetime, η was introduced into the damage model, and the evolution equations of creep damage and low-cycle fatigue damage could be modified as

$$d\tilde{D}_c = \eta \left(\frac{\sigma}{A} \right)^r (1 - \tilde{D})^{-m} dt \quad (11)$$

$$d\tilde{D}_f = \frac{1}{\eta} D_f = \frac{1}{\eta} \left(\frac{\sigma_a}{M} \right)^\beta (1 - \tilde{D})^{-b} dN \quad (12)$$

where \tilde{D}_c , \tilde{D}_f and \tilde{D} are creep damage, low-cycle fatigue damage and total creep-fatigue damage considering the effect of grain size, respectively. Therefore, the improved creep-fatigue damage model could be expressed as

$$\frac{d\tilde{D}}{dN} = (1 - \tilde{D})^{-m} \eta \int_{t_1}^{t_2} \left(\frac{\sigma}{A} \right)^r dt + (1 - \tilde{D})^{-b} \frac{1}{\eta} \left(\frac{\sigma_a}{M} \right)^\beta \quad (13)$$

3.2 Experimental verification of improved damage model

Creep-fatigue experiments of GH720Li superalloy with different grain sizes have been conducted in our previous work [36]. The main chemical compositions of GH720Li superalloy and the experimental conditions are shown in Table 2 and Table 3, respectively [36]. The specimens with different grain sizes were sampled from the center zone, middle zone and rim zone of the GH720Li turbine disc (Fig. 6). The experimental results indicated that, under the same conditions, creep-fatigue lifetimes increased with the increase of the grain size, while smaller grain sizes led to severer grain boundary cracking.

Using the damage-based lifetime prediction model developed in Section 2, the creep-fatigue

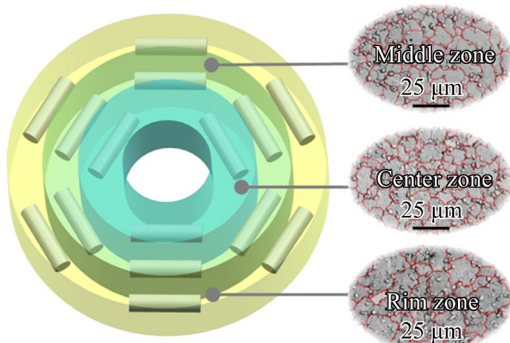
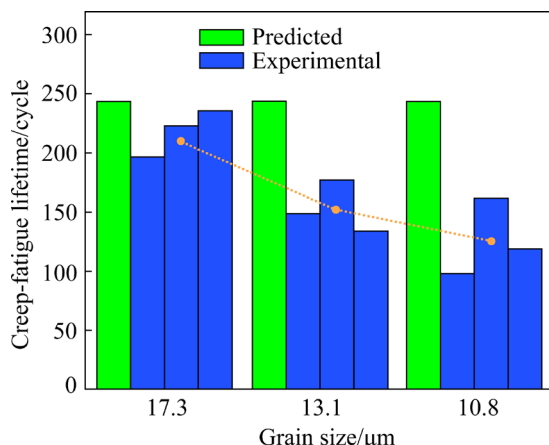
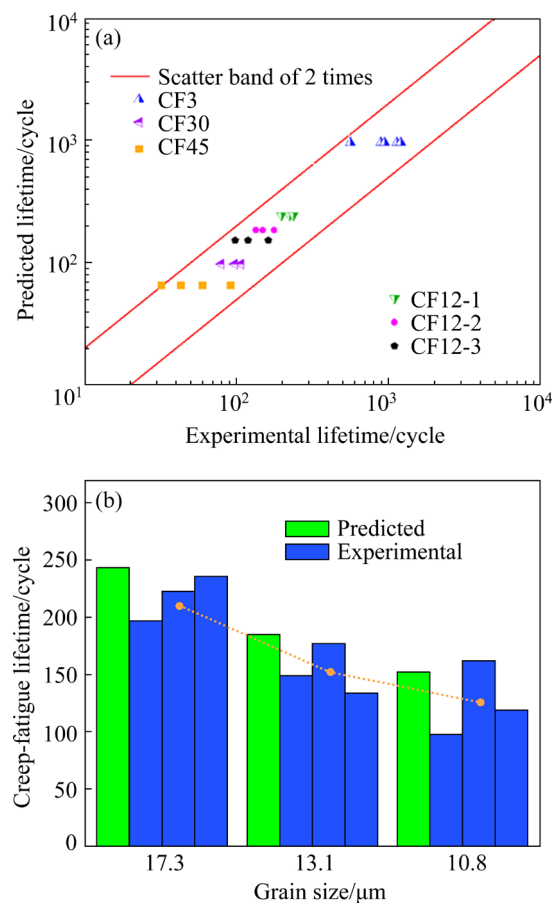
Table 2 Main chemical composition of GH720Li superalloy (wt.%) [36]

Cr	Co	Ti	Mo	Al	W	Fe	Si	Mn	Ni
15.50–16.50	14.00–15.50	4.75–5.25	2.75–3.25	2.25–2.75	1.00–1.50	≤0.50	≤0.20	≤0.15	Bal.

Table 3 Creep-fatigue experimental conditions of GH720Li superalloy [36]

Specimen ID	Temperature/°C	Stress ratio	Maximum stress/MPa	Dwell time/min	Grain size/μm	Number of specimens
CF12-1	650	0.1	1000	12	17.3	3
CF12-2	650	0.1	1000	12	13.1	3
CF12-3	650	0.1	1000	12	10.8	3

lifetime predictions for GH720Li superalloy with different grain sizes were conducted. Figure 7 illustrated that the lifetime prediction model failed to differentiate between the lifetimes of GH720Li superalloy specimens with different grain sizes. The creep-fatigue lifetime prediction results of GH720Li superalloy with different grain sizes based on the improved lifetime prediction model are shown in Fig. 8. Without introducing any additional material constants, the predicted creep-

**Fig. 6** Illustration of sampling locations on turbine disc**Fig. 7** Predicted creep-fatigue lifetimes of GH720Li superalloy with different grain sizes at 650 °C based on unimproved damage model**Fig. 8** Predicted creep-fatigue lifetimes of GH720Li superalloy with different grain sizes at 650 °C based on improved damage model (CF3, CF30 and CF45 indicate that dwell time at the maximum load is 3, 30 and 45 min, respectively): (a) Comparison between predicted lifetime and experimental lifetime; (b) Predicted laws between creep-fatigue lifetime and grain size

fatigue lifetimes of GH720Li superalloy at 650 °C fell within a scatter band of 2 times, and the relationship between creep-fatigue lifetimes and grain sizes was well described, verifying the rationality and accuracy of the grain-size-sensitive damage model developed in this work.

Disaster Prevention, Key Laboratory of Sichuan Province, China (No. FMEDP202305).

4 Conclusions

(1) Utilizing the nonlinear damage accumulation theory, the interaction between creep damage and low-cycle fatigue damage in creep-fatigue failure was characterized, leading to the development of a damage-based creep-fatigue lifetime prediction model for GH720Li superalloy.

(2) By fitting the experimental data of creep and low-cycle fatigue, the material constants for creep damage and low-cycle fatigue damage were identified. The predicted creep-fatigue lifetimes for GH720Li superalloy with an average grain size of $17.3 \mu\text{m}$ were essentially within a scatter band of 2 times, indicating a strong agreement between the predicted lifetimes and experimental data.

(3) Assuming that the influence of grain size on creep-fatigue damage was closely associated with the total grain boundary area, a grain-size-sensitive damage model for creep-fatigue was developed. Without introducing any additional material constants, the predicted creep-fatigue lifetime of GH720Li superalloy at 650°C fell within a scatter band of 2 times. Moreover, the predicted relationship between creep-fatigue lifetimes and grain sizes showed excellent agreement with the experimental data.

CRediT authorship contribution statement

Bin ZHANG: Investigation, Data curation, Writing – Original draft; **Rong-qiao WANG:** Writing – Original draft; **Dian-yin HU:** Writing – Review & editing; **Hong-bo LI, Kang-he JIANG, Jia-ming WEI** and **Hong ZHANG:** Formal analysis, Data curation.

Declaration of competing interest

The authors declare that they have no known competing financial interests or personal relationships that could have appeared to influence the work reported in this paper.

Acknowledgments

This work was financially supported by the National Natural Science Foundation of China (Nos. 52306183, 12272245, 11832007, 12172238), the Natural Science Foundation of Zhejiang Province, China (No. LQ23E050022), the Natural Science Foundation of Sichuan Province, China (Nos. 2022NSFSC0324, 2022JDJQ0011), and the Open Project of Failure Mechanics and Engineering

References

- [1] ZHANG Hong-kai, LI Yan, MA Teng-fei, CHANG Tian-xing, ZHANG Peng, FANG Xue-wei, HUANG Ke. Tailoring of nanoscale γ' precipitates and unveiling their strengthening mechanisms in multimodal nickel-based superalloy GH4720Li [J]. Materials Characterization, 2022, 188: 111918.
- [2] NING Yong-quan, WANG Tao, FU Ming-wang, LI Meng-nie, WANG Lin-feng, ZHAO C D. Competition between work-hardening effect and dynamic-softening behavior for processing as-cast GH4720Li superalloys with original dendrite microstructure during moderate-speed hot compression [J]. Materials Science and Engineering: A, 2015, 642: 187–193.
- [3] LIU Fang-fang, CHEN Jia-yu, DONG Jian-xin, ZHANG Mai-cang, YAO Zhi-hao. The hot deformation behaviors of coarse, fine and mixed grain for Udimet 720Li superalloy [J]. Materials Science and Engineering: A, 2016, 651: 102–115.
- [4] MUKHERJEE S, KUMAR KAR S, SIVAPRASAD S, TARAFDER S, VISWANATHAN G B, FRASER H L. Creep-fatigue response, failure mode and deformation mechanism of HAYNES 282 Ni based superalloy: Effect of dwell position and time [J]. International Journal of Fatigue, 2022, 159: 106820.
- [5] HU Dian-yin, MA Qi-hang, SHANG Li-hong, GAO Ye, WANG Rong-qiao. Creep-fatigue behavior of turbine disc of superalloy GH720Li at 650°C and probabilistic creep-fatigue modeling [J]. Materials Science and Engineering: A, 2016, 670: 17–25.
- [6] ZHANG Qing, ZUO Zheng-xing, LIU Jin-xiang. A model for predicting the creep-fatigue life under stepped-isothermal fatigue loading [J]. International Journal of Fatigue, 2013, 55: 1–6.
- [7] MARCHIONNI M, OSINKOLU G A, ONOFRIO G. High temperature low cycle fatigue behaviour of UDIMET 720 Li superalloy [J]. International Journal of Fatigue, 2002, 24: 1261–1267.
- [8] ONOFRIO G, OSINKOLU G A, MARCHIONNI M. Effects of loading waveform on fatigue crack growth of Udimet 720 Li superalloy [J]. International Journal of Fatigue, 2004, 26: 203–209.
- [9] RAI R K, SAHU J K. Mean-stress and oxidation effects on fatigue behaviour of CM 247 DS LC alloy [J]. Materials Science and Technology, 2019, 35: 1220–1226.
- [10] SILVA J M, CLÁUDIO R A, BRANCO C M, FERREIRA J M. Creep-fatigue behavior of a new generation Ni-base superalloy for aeroengine usage [J]. Procedia Engineering, 2010, 2: 1865–1875.
- [11] BILLOT T, VILLECHAISE P, JOUIAD M, MENDEZ J. Creep-fatigue behavior at high temperature of a UDIMET 720 nickel-base superalloy [J]. International Journal of Fatigue, 2010, 32: 824–829.
- [12] SHI Duo-qi, LIU Jin-long, YANG Xiao-guang, QI Hong-yu, WANG Jing-ke. Experimental investigation on low cycle

fatigue and creep-fatigue interaction of DZ125 in different dwell time at elevated temperatures [J]. *Materials Science and Engineering: A*, 2010, 528: 233–238.

[13] PENG He-li, LI Xi-feng, CHEN Xu, JIANG Jun, LUO Jing-feng, XIONG Wei, CHEN Jun. Effect of grain size on high-temperature stress relaxation behavior of fine-grained TC4 titanium alloy [J]. *Transactions of Nonferrous Metals Society of China*, 2020, 30: 668–677.

[14] QIN Jin, LI Zhi, MA Ming-yang, YI Dan-qing, WANG Bin. Diversity of intergranular corrosion and stress corrosion cracking for 5083 Al alloy with different grain sizes [J]. *Transactions of Nonferrous Metals Society of China*, 2022, 32: 765–777.

[15] REZAEI A H R, SHAYANPOOR A A. New constitutive equation utilizing grain size for modeling of hot deformation behavior of AA1070 aluminum [J]. *Transactions of Nonferrous Metals Society of China*, 2021, 31: 345–357.

[16] JACKSON M P, REED R C. Heat treatment of UDIMET 720Li: The effect of microstructure on properties [J]. *Materials Science and Engineering: A*, 1999, 259: 85–97.

[17] PANG H T, REED P A S. Microstructure effects on high temperature fatigue crack initiation and short crack growth in turbine disc nickel-base superalloy Udimet 720Li [J]. *Materials Science and Engineering: A*, 2007, 448: 67–79.

[18] CHEN Xiang, YANG Zhi-qing, SOKOLOV M A, ERDMAN D L, MO Kun, STUBBINS J F. Low cycle fatigue and creep-fatigue behavior of Ni-based alloy 230 at 850 °C [J]. *Materials Science and Engineering: A*, 2013, 563: 152–162.

[19] KIM T W, KANG D H, YEOM J T, PARK N K. Continuum damage mechanics-based creep-fatigue-interacted life prediction of nickel-based superalloy at high temperature [J]. *Scripta Materialia*, 2007, 57: 1149–1152.

[20] ZHANG Guo-dong, ZHAO Yan-fen, XUE Fei, MEI Jin-na, WANG Zhao-xi, ZHOU Chang-yu, ZHANG Lu. Creep-fatigue interaction damage model and its application in modified 9Cr–1Mo steel [J]. *Nuclear Engineering and Design*, 2011, 241: 4856–4861.

[21] ZHANG Bin, WANG Rong-qiao, HU Dian-yin, JIANG Kang-he, HAO Xin-yi, MAO Jian-xing, JING Fu-lei. Damage-based low-cycle fatigue lifetime prediction of nickel-based single-crystal superalloy considering anisotropy and dwell types [J]. *Fatigue & Fracture of Engineering Materials & Structures*, 2020, 43: 2956–2965.

[22] BERTI G A, MONTI M. Improvement of life prediction in AISI H11 tool steel by integration of thermo-mechanical fatigue and creep damage models [J]. *Fatigue & Fracture of Engineering Materials & Structures*, 2009, 32: 270–283.

[23] WANG Rong-qiao, ZHANG Bin, HU Dian-yin, JIANG Kang-he, HAO Xin-yi, MAO Jian-xing, JING Fu-lei. In-phase thermomechanical fatigue lifetime prediction of nickel-based single crystal superalloys from smooth specimens to notched specimens based on coupling damage on critical plane [J]. *International Journal of Fatigue*, 2019, 126: 327–334.

[24] GOSWAMI T. Low cycle fatigue-dwell effects and damage mechanisms [J]. *International Journal of Fatigue*, 1999, 21: 55–76.

[25] HALES R. A quantitative metallographic assessment of structural degradation of type 316 stainless steel during creep-fatigue [J]. *Fatigue & Fracture of Engineering Materials and Structures*, 1980, 3: 339–356.

[26] SKELTON R P, GANDY D. Creep-fatigue damage accumulation and interaction diagram based on metallographic interpretation of mechanisms [J]. *Materials at High Temperatures*, 2008, 25: 27–54.

[27] EDWARD G H, ASHBY M F. Intergranular fracture during power-law creep [J]. *Acta Metallurgica*, 1979, 27: 1505–1518.

[28] BOUCHARD P J, WITHERS P J, MCDONALD S A, HEENAN R K. Quantification of creep cavitation damage around a crack in a stainless steel pressure vessel [J]. *Acta Materialia*, 2004, 52: 23–34.

[29] XIAO Lin, CHEN Dao-lun, CHATURVEDI M C. Low-cycle fatigue behavior of INCONEL 718 superalloy with different concentrations of boron at room temperature [J]. *Metallurgical and Materials Transactions A*, 2005, 36: 2671–2684.

[30] WANG Run-zi, CHEN Hao, ZHANG Yang, ZHANG Xian-cheng, TU Shan-tung. Creep-fatigue life prediction in nickel-based superalloy GH4169 based on microstructural damage quantification with the help of electron backscatter diffraction [J]. *Materials & Design*, 2020, 195: 108939.

[31] KACHANOV L M. Time of the rupture process under creep conditions [J]. *Izvestiia Akademii Nauk SSSR, Otdelenie Tekhnicheskikh Nauk*, 1958, 8: 26–31.

[32] CHABOCHE J L. Continuous damage mechanics: A tool to describe phenomena before crack initiation [J]. *Nuclear Engineering and Design*, 1981, 64: 233–247.

[33] LEMAIRE J. How to use damage mechanics [J]. *Nuclear Engineering and Design*, 1984, 80: 233–245.

[34] ZHANG Bin, WANG Rong-qiao, LIU Hai-yan, HU Dian-yin, JIANG Kang-he, MI Dong, JING Fu-lei. Low cycle fatigue lifetime and deformation behaviour prediction of nickel-based single crystal superalloy considering thickness debit effect [J]. *Engineering Fracture Mechanics*, 2023, 281: 109076.

[35] High Temperature Materials Branch of Chinese Society of Metals. Chinese high temperature alloy handbook [M]. Beijing: Standards Press of China, 2012. (in Chinese)

[36] HU Dian-yin, GAO Ye, MA Qi-hang, SHANG Li-hong, WANG Rong-qiao. The effect of grain size on the creep-fatigue life of GH720Li superalloy [J]. *Rare Metal Materials and Engineering*, 2018, 47: 2386–2391. (in Chinese)

[37] GOODMAN J. Mechanics applied to engineering [M]. London: Longmans Green, 1899.

[38] NING Yong-quan, YAO Ze-kun, GUO Hong-zhen, FU Ming-wang. Structural-gradient-materials produced by gradient temperature heat treatment for dual-property turbine disc [J]. *Journal of Alloys and Compounds*, 2013, 557: 27–33.

[39] ZHANG Bao-yun, LIU Xiao-ming, YANG Hao, NING Yong-quan. The deformation behavior, microstructural mechanism, and process optimization of PM/wrought dual superalloys for manufacturing the dual-property turbine disc [J]. *Metals*, 2019, 9: 1127.

[40] DU Bei-ning, YANG Jin-xia, CUI Chuan-yong, SUN Xiao-feng. Effects of grain size on the high-cycle fatigue behavior of IN792 superalloy [J]. *Materials & Design*, 2015,

65: 57–64.

[41] MENG Zi-jie, ZHANG Cun-sheng, WU Cheng-ge, ZHANG Hao, CHEN Liang, ZHAO Guo-qun, YAN Hai. Low cycle fatigue behavior and fatigue life prediction of 2195 Al–Li alloy at warm temperatures [J]. Transactions of Nonferrous Metals Society of China, 2023, 33: 2574–2587.

[42] ZHANG Peng, ZHU Qiang, CHEN Gang, QIN He-yong,

WANG Cuan-jie. Grain size based low cycle fatigue life prediction model for nickel-based superalloy [J]. Transactions of Nonferrous Metals Society of China, 2018, 28: 2102–2106.

[43] ROHRER G S. Measuring and interpreting the structure of grain-boundary networks [J]. Journal of the American Ceramic Society, 2011, 94: 633–646.

考虑晶粒尺寸影响的 GH720Li 高温合金的蠕变–疲劳寿命预测

张 畝¹, 王荣桥^{2,3,4}, 胡殿印^{2,3,4}, 李洪波⁵, 蒋康河⁶, 魏佳明⁷, 张 宏⁸

1. 杭州市北京航空航天大学 国际创新研究院, 杭州 311115;
2. 北京航空航天大学 航空发动机研究院, 北京 100191;
3. 航空发动机结构强度北京市重点实验室, 北京 100191;
4. 中小型航空发动机联合研究中心, 北京 100191;
5. 清华大学 航天航空学院, 北京 100084;
6. 中国航发 湖南动力机械研究所, 株洲 412002;
7. 杭州汽轮动力集团股份有限公司, 杭州 310000;
8. 四川大学 灾变力学与工程防灾四川省重点实验室, 成都 610065

摘要: 为了准确评估 GH720Li 高温合金的蠕变–疲劳寿命, 建立了反映蠕变损伤与低循环疲劳损伤交互作用的寿命预测模型。平均晶粒尺寸为 $17.3 \mu\text{m}$ 的 GH720Li 高温合金的蠕变–疲劳寿命预测结果基本在 2 倍分散带内, 表明预测寿命与试验结果吻合良好。考虑到双性能涡轮盘的晶粒尺寸从边缘向中心逐渐减小, 通过引入晶界面积比, 建立了晶粒尺寸敏感的蠕变–疲劳寿命预测模型, 克服了大多数传统预测方法难以反映晶粒尺寸与蠕变–疲劳寿命关系的缺点。

关键词: 蠕变–疲劳; 寿命预测; GH720Li 高温合金; 晶粒尺寸; 损伤累积

(Edited by Wei-ping CHEN)